Title

CX3CR1-Expressing Myeloid Cells Regulate Host–Helminth Interaction and Lung Inflammation

Journal

Advanced Biology, 6(3)

ISSN

2701-0198

Authors

Kim, Sang Yong
Barnes, Mark A
Sureshchandra, Suhas
et al.

Publication Date

2022-03-01

DOI

10.1002/adbi.202101078

Peer reviewed

HHS Public Access

Author manuscript

Adv Biol (Weinh). Author manuscript; available in PMC 2023 March 01.

Published in final edited form as:

Adv Biol (Weinh). 2022 March ; 6(3): e2101078. doi:10.1002/adbi.202101078.

CX3CR1-expressing myeloid cells regulate host-helminth interaction and lung inflammation

Sang Yong Kim[ϒ],
Division of Biomedical Sciences, School of Medicine, University of California Riverside, Riverside, California 92521, United States

Mark A. Barnes[ϒ],
Division of Biomedical Sciences, School of Medicine, University of California Riverside, Riverside, California 92521, United States

Suhas Sureshchandra[ϒ],
Department of Molecular Biology and Biochemistry, School of Biological Sciences, University of California, Irvine, California 92697-3900, United States

Andrea R. Menicucci,
Department of Molecular Biology and Biochemistry, School of Biological Sciences, University of California, Irvine, California 92697-3900, United States

Jay J. Patel,
Division of Biomedical Sciences, School of Medicine, University of California Riverside, Riverside, California 92521, United States

Ilhem Messaoudi,
Department of Molecular Biology and Biochemistry, School of Biological Sciences, University of California, Irvine, California 92697-3900, United States

Meera G. Nair[*]
Division of Biomedical Sciences, School of Medicine, University of California Riverside, Riverside, California 92521, United States

Abstract

Many helminth life cycles, including hookworm, involve a mandatory lung phase, where myeloid and granulocyte subsets interact with the helminth and respond to infection-induced lung injury. To evaluate these innate subsets, we employ *Nippostrongylus brasiliensis* infection of reporter mice for myeloid cells ($CX3CR1^{GFP}$) and granulocytes ($PGRP^{dsRED}$). *Nippostrongylus* infection induces lung infiltration of reporter cells, including $CX3CR1^{+}$ myeloid cells and $PGRP^{+}$ eosinophils. Strikingly, $CX3CR1^{GFP/GFP}$ mice, which are deficient in CX3CR1, are protected from *Nippostrongylus* infection with reduced weight loss, lung leukocyte infiltration, and worm burden compared to $CX3CR1^{+/+}$ mice. This protective effect is specific for CX3CR1

[*]Correspondence: meera.nair@medsch.ucr.edu.
[ϒ]These authors contributed equally.

Supporting Information
Supporting Information is available from the Wiley Online Library or from the author.

as CCR2-deficient mice do not exhibit reduced worm burdens. *Nippostrongylus* co-culture with lung Ly6C$^+$ monocytes or CD11c$^+$ cells demonstrates that CX3CR1$^{GFP/GFP}$ monocytes secrete more proinflammatory cytokines, and actively bind the parasites causing reduced motility. RNA sequencing of Ly6C$^+$ or CD11c$^+$ cells shows *Nippostrongylus*-induced gene expression changes, particularly in monocytes, associated with inflammation, chemotaxis, and extracellular matrix remodeling pathways. We also identify cytotoxic and adhesion molecules as potential effectors against the parasite, such as *Gzma* and *Gzmb*, which are elevated in CX3CR1$^{GFP/GFP}$ monocytes. These studies validate a dual innate cell reporter for lung helminth infection and demonstrate that CX3CR1 impairs monocyte-helminth interaction.

Graphical Abstract

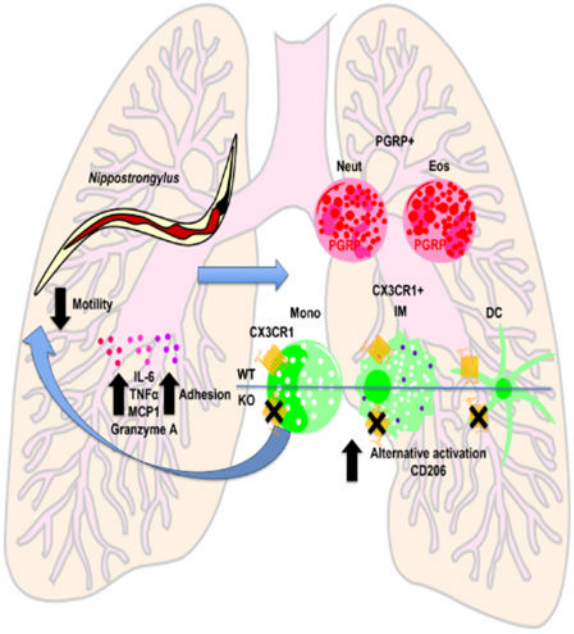

Keywords

helminth; innate immunity; chemokine receptor; macrophage

1. Introduction

Soil-transmitted helminths afflict over one billion individuals worldwide, where they can cause debilitating symptoms, including growth retardation, organ pathology and failure.[1] Given the development of anthelminthic drug resistance,[2] and the occurrence of re-infection after drug treatment,[3] understanding how to trigger protective immune effector responses offers valuable therapeutic insight to promote helminth elimination by the host. Helminths are macroparasites with complex life cycles that frequently involve tissue migration through many organs, leading to tissue pathology and inflammation.[4] Immune effector responses at these sites of incoming larval parasites are especially critical in preventing long-term infections. In particular, the lung is a main infection site for many

helminths, including hookworms *Necator americanus* and *Ancylostoma duodenale*, where the infectious larvae migrate through the lung as an essential developmental step before reaching the small intestine.[5]

While clinical symptoms of pulmonary helminth infection in humans have been reported, including coughing, wheezing, and potentially respiratory failure, investigation of the immune-mediated mechanisms within the lung against the helminth are less well understood, and rely on *in vivo* models such as murine helminth infection. One such murine model is infection with *Nippostrongylus brasiliensis*, a natural helminth parasite of rodents, which has a transient migratory phase through the lung prior to reaching the small intestine, mimicking pulmonary hookworm infection.[6] Previous studies have shown that pulmonary immune responses, including neutrophils and macrophages, are critical against *Nippostrongylus*.[7, 8] These studies utilized secondary challenge with *Nippostrongylus* to show that $CD4^+$ derived T helper type 2 cytokines and neutrophils promoted lung macrophage interaction and killing of *Nippostrongylus* larval parasites. The importance of other innate cells such as eosinophils have also been investigated, showing modest effects of eosinophils in promoting secondary effector responses to *Nippostrongylus*.[9] Eosinophil-dependent resistance was not required for resistance to the primary infection but was necessary for resistance to the secondary infection, which involves immobilizing worms and inhibiting their progression to the gut. These studies highlight the importance of innate effector cells in the lung, and prompted our study to investigate innate cells in *Nippostrongylus* infection. We focused on lung monocytes, which have been less well studied in lung helminth infection, although they are recruited and have important antimicrobial functions to a variety of other lung pathogens, and also can differentiate into dendritic cells and macrophages.[10] To this end, we investigated the CX3CR1 signaling pathway in influencing lung cell infiltration and activation in response to *Nippostronglyus* infection.

CX3CR1 is a G-protein coupled receptor that binds the chemokine CX3CL1/fractalkine. CX3CR1 is expressed on monocytes, where it is critical for effective monocyte adhesion and transmigration through the endothelium into the tissues. Within the tissue, and dependent on the inflammatory environment, CX3CR1-expressing monocytes differentiate into dendritic cells and macrophages, with essential protective functions against many pathogens, including bacteria and viruses.[11] CX3CR1 signaling also occurs in response to injury and fibrosis. In murine models of spinal cord injury and stroke, CX3CR1-deficient mice have ameliorated neural outcomes associated with a reparative phenotype in CX3CR1-expressing microglia and macrophages.[12] In pulmonary and peritoneal fibrosis models, CX3CR1 signaling is also detrimental, exacerbating fibrosis. Further, in infection with *Schistosoma japonicum*, acute hepatic granuloma formation and liver pathology is increased by CX3CR1 signaling, with little effect on parasite burdens.[13] Together, these studies suggest that CX3CR1 signaling is important for optimal effector responses to multiple pathogens, but needs to be tightly regulated to reduce inflammatory outcomes and tissue pathology. However, CX3CR1 signaling in pulmonary helminth infection has not previously been examined. We utilized CX3CR1-GFP knockout/knock-in transgenic mice to determine the kinetics of CX3CR1-expressing cells in the lung and investigate their role in infection with *Nippostrongylus brasiliensis*. To evaluate granulocyte lung subsets at the same time,

we generated dual reporters by crossing CX3CR1^{GFP} mice to reporter mice for PGRP-S, a peptidoglycan recognition protein identified in neutrophil granules.[14] Following *Nippostrongylus* infection, we observed CX3CR1^{GFP} and PGRP^{dsRed} cells in the lung and small intestine of infected mice. Flow cytometric characterization showed that these subsets were significantly increased at day 7 post-infection in the lung but not peripherally in the blood. The CX3CR1^{GFP} subsets were composed mainly of Ly6C^{+} monocytes and CD11c^{+} DCs, while the main PGRP^{dsRed} cells in the lung were eosinophils, identifying PGRP^{dsRed} mice as useful reporters to visualize and track eosinophils. Comparison of CX3CR1$^{+/+}$ and CX3CR1$^{GFP/GFP}$ mice revealed that CX3CR1-deficient mice were more protected against *Nippostrongylus* infection, associated with reduced infection-induced weight loss, lung leukocyte infiltration, and intestinal parasite burdens. In contrast, CCR2 deficiency did not show striking effects in *Nippostrongylus* infection. *Nippostrongylus* larval parasite co-culture with CD11c^{+} or Ly6C^{+} sorted from the infected lungs identified Ly6C^{+} monocytes as the functional downstream effectors in CXCR1-deficient mice, with increased expression of proinflammatory cytokines, and enhanced binding to the parasite, leading to reduced worm motility. RNA-seq analysis was performed on Ly6C^{+} monocytes and CD11c^{+} cells sorted from the infected lungs of CX3CR1$^{GFP/+}$ and CX3CR1$^{GFP/GFP}$ mice. The most differentially expressed genes was observed in Ly6C^{+} monocytes in response to infection, and the CX3CR1-deficient Ly6C^{+} monocytes demonstrated increased cytotoxic molecules and enhanced chemokines compared to CX3CR1$^{GFP/+}$ monocytes. In contrast, CD11c^{+} CX3CR1-expressing cells represented a heterogeneous macrophage/dendritic population with some infection-induced changes in gene expression but no significant gene expression changes between CX3CR1$^{GFP/+}$ and CX3CR1$^{GFP/GFP}$ CD11c^{+} cells. Together, these studies validate a dual reporter for myeloid and granulocyte subsets in *Nippostrongylus* infection, and identify a previously unrecognized role for CX3CR1 signaling in promoting infection-induced weight loss and leukocyte infiltration and impairing optimal effector responses to *Nippostrongylus*, in part through effects on monocytes.

2. Results

2.1. Dynamic changes in CX3CR1-expressing myeloid cells and PGRP-expressing eosinophils in the helminth-infected lung.

The transgenic reporter GFP knock-in/knock out CX3CR1 (*Cx3cr1*) mouse offers the opportunity to track myeloid cells and investigate the function of CX3CR1 signaling,[15] while the dsRedPGRP-S (*Pglyrp1*) mice, in which the dsRed transgene, under the control of the *Pglyrp1* promoter, is integrated into the genome, are reporters for a peptidoglycan recognition protein present in neutrophil granules.[14, 16] We generated dual reporter transgenic mice, CX3CR1$^{GFP/+}$PGRP^{dsRed} to determine their utility in tracking innate cells in helminth infection. Immunofluorescent imaging of lung and small intestine cryosections demonstrated strong GFP and dsRed signal in cells within the lung parenchyma and lamina propria of the small intestine (Figure 1A). Comparison of cryosections from naive or day 7 post-*Nippostrongylus* infection, when the adult parasites are present in the small intestine,[17] revealed infection-induced infiltration of reporter cells. This was particularly evident in the lung, reflecting the inflammatory response to the transient migration (day 2–3 post-infection) of the helminth parasites, which is evident even after the parasite

has left the lung (day 3–4 post-infection). CX3CR1-positive cells were increased in the infected lungs but not the intestine, while PGRP-positive cells were increased in the lung and to a lesser extent in the small intestine. Given that these innate reporter cell subsets had not previously been investigated in pulmonary helminth infection, we utilized flow cytometry to characterize these subsets in the lung and determine their kinetics over the course of helminth infection. Flow cytometric analysis of single-cell suspensions from naive or infected $CX3CR1^{GFP/+}PGRP^{dsRed}$ mice showed distinct single and double GFP/dsRed positive cells following infection (Figure 1B). Further gating and overlay with reporter negative wild-type (WT) mice revealed that the double-positive cells were in fact artifacts consisting of autofluorescent alveolar macrophages (Figure 1B, Figure S1A–C). This is consistent with prior studies showing that alveolar macrophages do not express CX3CR1, [15] therefore we gated out these cells in subsequent analysis. The $CX3CR1^{+}$ cells from the infected lungs were composed of three main subsets: $CD11c^{+}$ dendritic cells (DC), interstitial macrophages (IM), and $Ly6C^{+}$ monocytes with minimal contributions from $CD3^{+}$ T cells and $NK1.1^{+}$ Natural Killer (NK) cells (Figure S1D).

PGRP is reported to be a granule protein found in neutrophils and M cells.[14, 16] Unexpectedly, we observed that most of the $PGRP^{+}$ cells in the infected lung, especially at day 7 post-infection were in fact eosinophils, followed by neutrophils (Figure 1B and S1C). To evaluate if the reporter protein was effective for live cell imaging, lung cells were isolated from *Nb*-infected $CX3CR1^{+/+}PGRP^{Neg}$, $CX3CR1^{+/+}PGRP^{DsRed}$, and $CX3CR1^{+/GFP}PGRP^{DsRed}$ mice and co-cultured with *Nb* L3 larvae. CX3CR1 and PGRP single-positive cells exhibited strong signal and bound to the larvae suggesting that these reporter mice are also a valuable tool to image myeloid and granulocyte subsets (Fig 1C).

Flow cytometry analysis at various timepoints post-infection showed that both $CX3CR1^{+}$ cells and $PGRP^{+}$ cells peaked at day 7 post-infection in the lung (Figure 2A). The frequency of $CX3CR1^{+}CD11c^{+}$ cells in the lung increased 11 times (1% to 11%), and $CX3CR1^{+}$ monocytes increased 2.5 times (2% to 5%) at day 7 post-infection compared to naive mice. Lung eosinophils in the $PGRP^{+}$ cell subset were also significantly increased (5-fold) at day 7 post-infection, but there were no significant differences in the frequency of these cells in the blood (Figure 2A), indicating that infection-induced changes in these subsets occurred mostly at the infection site. These significant changes in eosinophils and $CX3CR1^{+}$ myeloid cells were transient, with recovery to naive frequencies at day 10 post-infection. Together, this data shows dynamic changes in lung innate effector cells in response to helminth infection. These included significant but transient increases in myeloid cells and eosinophils, which can be efficiently tracked by transgenic mouse reporters for CX3CR1 and PGRP respectively.

2.2. CX3CR1-deficient mice show improved outcomes to *Nippostrongylus* infection.

To determine the role of CX3CR1 signaling in helminth infection, wild-type (WT) and $CX3CR1^{GFP/GFP}$ (KO) mice were infected with *Nippostrongylus*. Both WT and KO mice exhibited infection-induced weight loss at days 2 and 3 post-infection (Figure 3A), consistent with the pathologic consequence of parasite migration through the lung. However, KO mice had ameliorated outcomes with significantly reduced infection-induced weight loss

compared to WT mice. Since a higher weight loss is typically associated with stronger inflammatory responses, the number of immune cells in the lung was enumerated (Figure 3B). Consistent with the reduced weight loss, lung leukocyte counts were significantly lower in KO mice. Different immune cell populations in the lung were analyzed by flowcytometry, and monocytes, alveolar macrophages, and $CD11c^+$ cells were significantly decreased in infected KO mice, which is consistent with the importance of CX3CR1 signaling for myeloid subset recruitment (Fig 3C). Although there was a significant increase in eosinophil frequency in KO mice, there were no differences in lung eosinophil or neutrophil numbers between WT and KO mice. The expression of CD206 (mannose receptor), a surrogate for M2 macrophage activation[18], was significantly increased in alveolar macrophages and in $CD11c^+$ cells from KO mice compared to WT mice, suggesting increased M2 polarization in the absence of CX3CR1 signaling. M2 polarized macrophages are important effector cells against lung migrating larvae such as *Nippostrongylus*,[4, 7] therefore we tested the hypothesis that KO mice may have improved innate responses to *Nippostrongylus* leading to reduced parasite burdens. Intestinal worm counts at day 7 post-infection confirmed an almost 3-fold decrease in worm burdens and an 8-fold decrease in fecal egg counts (Figure 3D). This was associated with decreased parasite viability, measured by ATP quantification of adult worms recovered from the intestine.

We tested whether this protective effect was specific for CX3CR1 deficiency, or if deficiency in myeloid cell recruitment through another chemokine receptor such as CCR2, also resulted in lower lung leukocyte infiltration and parasite burdens. CCR2 deficiency ($CCR2^{RFP/RFP}$) did not have any significant effect on infection-induced weight loss or worm burden (Figure S2A, B). This was despite significantly reduced lung leukocyte numbers and strikingly decreased infiltration of monocytes (33-fold) (Figure S2C), which validated the mice and confirmed that monocyte responses were CCR2-dependent. Additionally, CCR2 deficiency resulted in reduced frequency and numbers of alveolar macrophages, which may reflect deficiencies in monocyte-derived alveolar macrophages which have been identified in response to lung infection.[19] Nonetheless, we observed significantly increased surface expression of CD206 in CCR2-deficient alveolar macrophages suggesting that CCR2 deficiency, similar to CX3CR1 deficiency, may also cause M2 macrophage activation. We validated the CCR2 reporter, showing that $Ly6C^+$ monocytes were RFP-positive (Figure S2D). Thus, deficiency in CCR2 signaling did not significantly affect worm clearance although this receptor was important for recruiting monocytes and influenced macrophage M2 polarization. In contrast, CX3CR1 signaling had an unexpected and detrimental role in helminth infection, where it promoted lung myeloid cell responses and infection-induced pathology, but impaired M2 macrophage activation and optimal worm clearance.

2.3. CX3CR1-deficient $Ly6C^+$ monocytes are more active against the *Nippostrongylus* parasites and secrete more proinflammatory cytokines.

Both CCR2 and CX3CR1 deficiency led to decreased myeloid cell recruitment in the lung, however, the reduced parasite burden in CX3CR1 KO mice suggests that CX3CR1 signaling may have functional effects beyond its chemotactic function that impairs the innate immune response to parasitic worms. Given that $Ly6C^+$ monocytes and $CD11c^+$ myeloid cells were the main $CX3CR1^+$ cells in the lung at day 7 post-infection (see Figure 1), we investigated if

CX3CR1 deficiency in these subsets affected their effector function against *Nippostrongylus* parasites. In *in vivo* infection, *Nippostrongylus* infectious L3 larvae migrate to the lung triggering innate effector cells, therefore we investigated this lung cell interaction *in vitro* by co-culture of lung cells with *Nippostrongylus* L3 parasites based on previously established methodologies.[20] $CD11c^+$ and $Ly6C^+$ cells were enriched by magnetic bead purification of dissociated lung cells from day 7-infected CX3CR1 WT and KO mice followed by co-culture with L3 *Nippostrongylus* larvae (Figure 4A). Microscopic visualization of co-cultures at day 3 revealed that both WT and KO $CD11c^+$ cells were effective at binding the larval parasite. In comparison, WT $Ly6C^+$ monocytes showed minimal larval binding, while KO $Ly6C^+$ monocytes exhibited strikingly increased adherence to the worm (Figure 4B). Quantification of cell numbers per worm confirmed a more than 4-fold increase in binding of KO $Ly6C^+$ compared to WT $Ly6C^+$ monocytes, with no significant difference between WT and KO $CD11c^+$ cells (Figure 4C). We evaluated the outcome of enhanced cell binding by quantifying larval motility, and confirmed that co-culture with cells from all four groups led to reduced larval motility compared to larvae cultured alone. Co-culture with $Ly6C^+$ KO monocytes resulted in significantly reduced larval motility compared to WT monocytes, consistent with more efficient binding to the worm. Measurement of proinflammatory cytokines in the co-culture supernatants revealed that KO monocytes secreted 10-fold more TNFα and IL-6, and 20-fold more MCP-1 than WT monocytes (Figure 4D). In contrast, there was no difference between WT and KO $CD11c^+$ cells, nor differences in secretion of IFNγ, IL-10 or IL-12 in any of the groups (data not shown). We investigated if addition of live *Nippostrongylus* larvae was necessary for this cytokine production by lung cells in the co-culture, but observed that there were no significant differences in cytokine production between lung cells alone, or cells incubated with *Nippostrongylus* larvae (Figure 4E and data not shown). Together, our data indicate that CX3CR1 deficiency has targeted effects on monocytes infiltrating the helminth-infected lung, including increased proinflammatory cytokines and adherence to the parasite, which leads to improved effector responses against the parasite.

2.4. RNA expression profiling of $Ly6C^+$ and $CD11c^+$ subsets reveals *Nippostrongylus*-induced and CX3CR1-dependent changes particularly in lung $Ly6C^+$ monocytes

Our previous data identified an unexpected role for CX3CR1 signaling in the lung in impairing effector responses to helminth parasites, therefore we investigated potential differences between $CX3CR1^{+/GFP}$ (Het) and $CX3CR1^{GFP/GFP}$ (KO) lung by RNA-sequencing analysis, focusing on $Ly6C^+$ and $CD11c^+$ cells as the main CX3CR1-expressing subsets in the lung. $PGRP^+CX3CR1$ Het and KO mice were infected with *Nippostrongylus* L3, and we validated, as before, reduced parasite burden and lung leukocyte counts in the KO mice (Figure S3A). To determine infection-induced changes in the CX3CR1-expressing subsets, we also examined PBS-treated Het mice. At day 7 post *Nippostrongylus* infection, $CX3CR1^+GFP^+$ subsets were sorted based on Figure 5A, where the gating strategy included removing $PGRP^+$ cells to minimize contamination from granulocytes and alveolar macrophages. We evaluated gene expression changes between naïve and infected groups, $CD11c^+$ and $Ly6C^+$ cells, and CX3CR1-Het and KO genotype. $Ly6C^+$ cells exhibited the most differential gene expression according to infection status (naïve vs infected, n=180) and according to genotype (CX3CR1 Het vs KO, n=20) (Figure 5B). Functional enrichment

of differentially expressed genes in CX3CR1-expressing Ly6C$^+$ monocytes from naïve or infected lungs revealed that *Nippostrongylus* infection was associated with changes in genes involved with migration (e.g. regulation of cell migration, monocyte chemotaxis), inflammation (e.g. inflammatory response, cellular response to TNF), and tissue remodeling (e.g. collagen fibril organization, angiogenesis, ECM receptor interaction) (Figure 5C, D). Heatmap of the most differentially expressed genes in monocytes following infection suggests infection-induced increases in chemokines (*Ccl12, Ccl24, Ccl7, Cxcl16*) and matrix metalloproteinases (*Mmp14, Mmp19, Timp1*), indicating that monocytes were involved in promoting leukocyte recruitment to the infected tissue and in tissue remodeling (Fig 5E). In contrast, several collagen-encoding genes were downregulated upon infection (*Col1a1, Col1a2, Col14a1*), suggesting decreased function in collagen matrix deposition.

When comparing Cx3CR1 Het and KO Ly6C+ monocytes sorted from infected lungs, most DEG were upregulated in Ly6C$^+$ KO cells, and indicated enhanced chemotactic and cytotoxic responses. These included *Ugcg*, *Sh2d2a, Eomes*, *Gzma* and *Gzmb*, which are associated with innate and adaptive effector cell responses, especially cytotoxic NK and CD8 T cell function.[21] y6C$^+$ KO cells expressed significantly decreased *Maged1*, a gene identified in NK cells which triggers cell death. Downregulation of this gene may suggest the increased longevity of the CX3CR1-deficient monocytes.[22]. *Ets1*, which mediates vascular inflammation and remodeling, was upregulated in KO Ly6C$^+$ cells. Ets-1 is a known activator of CCL2, which supports the increased monocyte activity in the co-culture data.[23] Unexpectedly, *Ccl3* was also significantly reduced in KO Ly6C$^+$ cells, which is in contrast to the significantly upregulated secretion of another chemokine, MCP-1/CCL2, in the co-cultures. This result may reflect differences between RNA and protein levels, the different chemokines, or differences between the *in vivo* versus *in vitro* environment. Cytotoxic genes are usually expressed in CD8 and NK cells and not typically in monocytes, however, the flow cytometry characterization suggested that Ly6C$^+$CX3CR1-expressing subset had minimal contamination from these cytotoxic effector subsets (see Figure S1C). To investigate this further, we utilized ImmQuant for digital cell quantification of the RNA-seq datasets based on the immunological genome (Figure S4).[24] Overall, the top cell hits for the sorted Ly6C$^+$ subsets were monocytes from various lymphoid tissues. Although most of the datasets used for ImmQuant reflect naive conditions and lymphoid organs, these findings support our sorting strategy for monocytes. While Ly6C$^+$ cells from infected Het mice did not show similarities to NK nor CD8 T cells, KO Ly6C$^+$ cells matched NK and CD8 T cell subsets, albeit at a lower score than that for monocytes. It is possible that the Ly6C$^+$ KO cells may be monocytes that acquire NK and CD8 T cell cytotoxic characteristics in the absence of CX3CR1 signaling. Alternatively, there may be more contamination of CD8 and NK cells in the KO subset. Despite these caveats, our data indicate that CX3CR1 deficiency promotes cytotoxic functions, which may be linked to the improved immunity and damage to the *Nippostrongylus* parasites.

Compared to monocytes, there were minimal gene expression changes in CD11c$^+$ cells, with only 65 DEG between naïve and infected groups, and no significant DEG were found between CX3CR1 Het and KO cells (Figure S3). These findings may reflect the greater heterogeneity in the CD11c$^+$ lung subsets, which would mask any significant gene expression changes. Additionally, there was no functional difference between Het and

KO CD11c+ cell when co-cultured with *Nb* larvae (see Figure 4). ImmQuant analysis of the CD11c$^+$ subsets supported a heterogeneous subset with gene expression profiles that matched both DCs and macrophages from a variety of tissues including the lung (Figure S4). Comparison of DEG between Het CD11c+ cells sorted from naïve and infected lungs indicated most DEG were downregulated genes in infection (52 downregulated vs 13 upregulated). Downregulated genes were associated with proliferation (*Pou2f2*),[25] anti-inflammatory function (*CD300e*),[26] and cell adhesion (*Itga1*, *Itgb7*), suggesting that the CD11c$^+$ subset was more quiescent in the infected lungs. Interestingly, CD11c$^+$ cells from infected lungs also had reduced expression of the angiotensin-converting enzyme *Ace*, which has been reported to in pulmonary granuloma formation.[27]

Overall, these results demonstrate that *Nippostrongylus* infection induces gene expression changes, especially in CX3CR1-expressing lung monocytes, associated with chemokines, inflammation, and matrix remodeling pathways. These data also identify candidate cytotoxic and adhesion molecules as effectors against the parasite.

3. Discussion

The overall goals of this study were to characterize innate effector lung cells in response to *Nippostrongylus* infection, and to determine the function of chemokine receptor signaling through CX3CR1 and CCR2 in infection-induced inflammation and parasite clearance. Using dual reporters for CX3CR1 and PGRP, we show that CX3CR1-expressing monocytes and dendritic cells are induced in the *Nippostrongylus*-infected lungs, and identify the significant infection-induced infiltration of PGRP^{dsRed} eosinophils. We found that eosinophils have strong PGRP^{dsRed} signal that can be detected by fluorescence microscopy and flow cytometry, suggesting that this transgenic model may be useful to visualize eosinophils. PGRP proteins are critical innate sensors of bacterial peptidoglycan, triggering innate signaling to promote microbicidal responses.[28] Prior to these studies, PGRP expression in mice had been reported in the granules of neutrophils and M cells.[14, 16] However, a bovine study reported expression in eosinophils,[29] which is in line with our findings. In that study, PGRP was microbicidal against the fungal pathogen *Cryptococcus* and gram-negative bacteria in which peptidoglycan was buried (*Salmonella*), suggesting a potential function for these proteins that may not be mediated by peptidoglycan recognition. Beyond its utility as a reporter for eosinophils and neutrophils, investigation of PGRP effector responses against helminth parasites may be warranted.

We investigated chemokine receptor signaling through CX3CR1 and CCR2, which are expressed in monocytes.[15, 30] Monocytes infiltrate tissues in response to infection and injury, and have critical roles in various microbial infections, including viral, bacterial and protozoan.[10, 31] However, few studies have investigated monocyte responses in helminth infection, or monocyte-helminth interaction. Here we identify both chemotactic and non-chemotactic functions for CX3CR1-expressing monocytes in *Nippostrongylus* infection. Deficiency in CX3CR1 signaling led to reduced lung leukocyte infiltration, with reductions in monocyte and DC subsets, consistent with these cells requiring CX3CR1 for recruitment to inflamed tissues.[15, 32] Although lung alveolar macrophages do not express CX3CR1, they were also reduced in CX3CR1-deficient mice. In influenza infection studies, infiltrating

monocytes differentiate into alveolar macrophages, referred to as monocyte-derived alveolar macrophages, which then downregulate CX3CR1 expression.[33] It is possible that the reduction in alveolar macrophages in *Nippostrongylus*-infected CX3CR1-deficient mice may reflect reduction in these monocyte-derived subsets.

Functionally, CX3CR1-deficient mice exhibited ameliorated outcomes to *Nippostrongylus* infection, including reduced infection-induced weight loss, and significantly reduced parasite burdens. This protective effect was not observed in CCR2-deficient mice, although these mice also had reduced monocyte and alveolar macrophage frequencies in the lung, consistent with the CCR2-mediated chemotaxis. These data therefore suggest a non-chemotactic function for CX3CR1 that is distinct from CCR2. Functional differences between CCR2 and CX3CR1 are supported by prior studies showing that inflammatory monocytes have high CCR2, while resident monocytes, as well as macrophages and DC in specific tissues, express CX3CR1.[34] Overall, there is general consensus that CCR2 is specific for inflammatory monocytes, while CX3CR1 is expressed on anti-inflammatory macrophages.[35] Related to our findings, a study investigating pulmonary hypoxia reported that CX3CR1 deficiency was protective against hypoxia while CCL2 deficiency had no effect.[36] In our study with lung helminth infection, we observed that CX3CR1-deficient $Ly6C^+$ monocytes were more effective at migrating and binding to the *Nippostrongylus* larvae, and also secreted higher levels of proinflammatory cytokines. These findings indicate an inhibitory function for CX3CR1 in suppressing effector responses in monocytes, and suggest that therapeutically targeting CX3CR1 signaling may enhance immunity to helminths through promoting tissue monocyte responses. In viral and fungal parasite infection, CX3CR1 signaling is protective for pathogen killing,[32, 37] yet in our studies with helminth infection, CX3CR1 signaling impaired parasite clearance and was associated with reduced M2 macrophage activation. It is possible that CX3CR1 signaling influences the balance between M1/M2, favoring M1 macrophage activation instead of anti-helminthic M2 macrophage responses. Studies in neural tissue injury showed that CX3CR1 signaling exacerbates inflammation and CX3CR1 KO macrophages show a reparative phenotype.[12] This is consistent with our findings, where we show that CX3CR1-deficient cells have higher expression of M2 marker CD206. Other studies in the lung investigated the function of CX3CR1 signaling in response to hypoxic pulmonary tension or bleomycin-induced fibrosis,[36, 38] which trigger similar pathways and share disease etiologies with *Nippostrongylus* infection of the lungs.[6] Consistent with our findings, those studies showed that CX3CR1 deficiency led to increased inflammatory cytokines (CCL2, TNFα), however, they noted a shift from M2 to M1 macrophage polarization in CX3CR1-deficient mice. This highlights the complex role of CX3CR1 signaling in the lung, which may depend on the inflammatory context and stressor (e.g., hypoxia, chemical, infection).

To identify candidate downstream effectors of CX3CR1 signaling that regulate host-helminth interaction, we conducted RNA-seq on $CX3CR1^{GFP}$ positive $Ly6C^+$ and $CD11c^+$ cells sorted from the lungs of CX3CR1 Het or deficient mice. We found that the greatest changes in gene expression occurred in $Ly6C^+$ monocytes in response to *Nippostrongylus* infection, which were associated with pathways involved in chemotaxis, inflammation and extracellular matrix receptor interaction. These data indicate dynamic changes in monocytes recruited to the lung in response to helminth infection, where they secrete chemokines and

cytokines as a positive feedback loop to enhance tissue inflammation. These monocytes are also likely involved in interaction with other immune cells as well as the matrix, as a response to injury. Based on studies in other infection models,[31] these monocytes may also differentiate into macrophages and dendritic cells with functions that are distinct from the tissue-resident subsets. We evaluated CX3CR1-dependent gene expression in Ly6C^{+} monocytes, and found that CX3CR1 deficiency led to expression of genes associated with NK and CD8 T cells. We cannot exclude the possibility of contamination from these cell-types, however, this data indicates CX3CR1 deficiency leads to an exacerbated cytotoxic effector function, such as the increased expression of granzymes (*Gzma* and *Gzmb*) and *Serpinb9*. Granzyme A caused membrane damage-mediated cell death, cleavage of many intracellular substrates,[39] and promotes proinflammatory cytokine expression, making it a candidate effector molecule for the enhanced effector response to *Nippostrongylus* observed in the CX3CR1-deficient mice. Granzyme B was shown to be upregulated in human monocytes by activation of TLR8 signaling and induced antibody-dependent cellular cytotoxicity.[40] *Serpinb9*, an endogenous natural antagonist regulating excessive granzyme B activity was also upregulated in KO monocytes, indicating potential regulation of this pathway.[41] Granzyme expression has been reported in both human and rodent helminth infections,[42] with divergent roles in the inflammatory response and anti-helminthic immunity. In infection with filarial nematode *Litomosomoides sigmodontis*, granzyme A deficiency increased susceptibility while deficiency in granzyme B promoted early inflammation and improved resistance.[43] Future experiments investigating the interplay between these effectors and regulators of the granzyme pathway, and how they might contribute to the enhanced cell binding to the larval parasite, may uncover new pathways that can be targeted to promote helminth killing. In conclusion, our study characterizes a dual reporter for innate myeloid and granulocyte subsets in pulmonary helminth infection, and identify a previously unrecognized role for CX3CR1 signaling in promoting infection-induced pathology and impairing optimal anti-helminth effector responses.

4. Experimental Section/Methods

Animals

The following studies were performed using eight to ten weeks old mice. CX3CR1^{GFP}/PGRP-S^{dsRed} double transgenic mice were generated as previously described,[16] and maintained in vivaria at the University of California Riverside (UCR). Briefly, GFP-expressing Cx3cr1^{tm1Litt} mice from Jackson Laboratory (Bar Harbor, ME) were crossed with PGRP-S dsRed transgenic mice. Colonies of wild-type C57BL/6 and RFP-expressing transgenic Ccr2$^{tm2.1Ifc}$ mice were obtained from Jackson Laboratory and maintained in UCR vivaria. CX3CR1^{GFP}/CCR2^{RFP} mice were generated by crossing Cx3cr1^{tm1Litt} mice and Ccr2$^{tm2.1Ifc}$ mice, originally obtained from Jackson Laboratory. All animal procedures were approved by the UCR Institutional Animal Care and Use Committee https://or.ucr.edu/ori/committees/iacuc.aspx; protocol A-20180023.

Nippostrongylus brasiliensis (Nb) culture, infection, and ATP assay

Nb life cycle was maintained in Sprague-Dawley rats obtained from Harlan Laboratories (Indianapolis, IN). L3 stage infective *Nb* larvae were extracted from feces of previously

infected rats. Mice were subject to subcutaneous injection of 500 L3 *Nb* or PBS for naïve groups. Mice were euthanized and tissue was harvested at days 3, 4, 7, 10, and 29 post-infection. *Nb* eggs in feces of infected mice were quantified using a McMaster chamber between days 6–10 after infection. To enumerate and extract L5 stage *Nb*, small intestines of infected mice were cut longitudinally and incubated in PBS for ≥ 2 hours at 37°C. Following extraction from the small intestine *Nb* were washed 3 times, then homogenized in PBS. ATP levels were quantified in *Nb* homogenates using CellTiter-Glo Luminescent Cell Viability Assay (Promega; Madison, WI), according to the manufacturer's instructions.

Immunofluorescence

Lungs were inflated through the trachea with a solution containing ⅓ 1% PFA/30% sucrose and ⅔ optimal cutting temperature (OCT) compound (Sakura Finetek USA; Torrance, CA), then placed in 4% PFA/30% sucrose for 2 hours at room temperature. Following fixation, lung tissue was embedded into OCT and sectioned at 10μm. Lung sections were treated overnight with StartingBlock Blocking Buffer (ThermoFisher Scientific; Waltham, MA). Endogenous GFP and DsRed were visualized in mounting medium with DAPI (VECTASHIELD; Burlingame, CA) using a 20x objective on an epifluorescent microscope.

Flow cytometry analysis and cell sorting

Lung tissue was minced, then incubated with 30μg/mL DNAse I (Sigma-Aldrich; St Louis, MO) and 1mg/mL Collagenase/Dispase (Roche Diagnostics; Indianapolis, IN) for 30 minutes in a 37°C shaking incubator. Single-cell suspensions were obtained by passing digested tissue over a 70μm cell strainer. Whole blood was collected from the mesenteric vein and mixed with 4% Sodium citrate. Leukocytes were separated from whole blood using Histopaque 1077 (Sigma-Aldrich). Cells were blocked with 25μg/mL of Rat IgG and anti-CD16/32 (clone 2.4G2; BD Biosciences; San Jose, CA), then stained for flow cytometry analysis with CD11b (M1/70), CD11c (N418), F4/80 (BM8), Ly6C (HK1.4), MHC II (AF6-120.1), NK1.1 (PK136) from eBioscience (San Diego, CA); CD206 (MR5D3) from Bio-Rad (Hercules, CA); biotinylated Siglec F from R&D Systems (Minneapolis, MN); and CD3 (145-2C11), CD4 (RM4-5), Ly6G (IA8) from BD Biosciences (San Jose, CA). For flow cytometry cell sorting, cells were blocked as above and stained with CD11c and Ly6C. Data for analysis were collected using an LSRII (Becton Dickinson; Franklin Lakes, New Jersey); sorted cells were collected using FACSAria (Becton Dickinson), with over 90% purity of the post-sorted cells. Data were analyzed using FlowJo v10.7.1 (Tree Star, Ashland, OR).

RNA Sequencing Bioinformatics Analysis

Flow cytometry-sorted cells were collected in RLT buffer (Qiagen; Hilden, Germany), and RNA was extracted and DNAse-treated using RNeasy Mini Kit (Qiagen) according to the manufacturer's protocol. cDNA libraries were synthesized using Clontech SMARTer Stranded RNA-Seq kit (Mountain View, CA) with multiplexing primers. Quality of RNA and cDNA libraries were analyzed using 2100 BioAnalyzer (Agilent Technologies; Santa Clara, CA), then samples were sequenced with Illumina HiSeq2500 (San Diego, CA). Quality reports of RNA-Seq reads were generated using FASTQC (version 0.11.5), and reads were trimmed using TrimGalore (version 0.4.1) (http://

www.bioinformatics.babraham.ac.uk/projects/trim_galore/) ensuring a minimum Phred Quality Score of at least 20, read lengths of at least 50 base pairs and removing any remaining adapters. The trimmed reads were then aligned to *Mus musculus* genome (GRCm38) from Ensembl using splice aware short read aligner Bowtie2/TopHat in a strand-specific manner.[44] Gene level counts were summarized based on Ensembl gene annotations (GRCm38.84) using GenomicRanges package in R,[45] counting reads that align to exonic regions only. Raw gene expression data have been submitted to NCBI GEO (SRA Project PRJNA744529). Differential gene expression (DEG) analysis was performed using edgeR package in R.[46] Briefly, genes with 0 counts in more than 50% of samples analyzed (lowly expressed genes) were excluded from differential testing. Data were normalized using TMM (Trimmed Mean of Means) normalization to account for compositional differences in libraries. Overall dispersion and differential metrics were computed using negative binomial GLM (Generalized Linear Models) functions in edgeR. DEGs were defined as those with fold change ≥ 1 and a false discovery rate (FDR) of ≤ 5%. Heatmaps were generated after normalizing raw counts using the RPKM (Reads Per Kilobase per Million Mapped Reads) method.[47] Functional enrichment of these DEGs was completed using DAVID Functional Annotation Tools to identify over-representative gene ontologies (GO) and KEGG pathways of interest (FDR ≤ 5%).[48]

In vitro Nb motility and cellular adherence, and cytokine quantification

$Ly6C^+$ and $CD11c^+$ cells from Nb-infected lungs of $CX3CR1^{+/+}$ and $CX3CR1^{GFP/GFP}$ were enriched with magnetic assisted cell sorting (MACs) using biotinylated Ly6C (HK1.4; Abcam) and Streptavidin microbeads, or CD11c microbeads (Miltenyi Biotech; San Diego, CA), which resulted in ~70% purity. 0.25×10^6 cells were plated in 48 well plates with 25 L3 stage *Nb* in the presence of 1:50 serum from the day 7 infected corresponding mouse group (WT serum for WT cells and KO serum for KO cells) according to previously reported methodologies.[20] Cells and *Nb* larvae were co-cultured for 4 days at 37°C. *Nb* motility was assessed as previously described,[20, 49] and cellular adherence was quantified by counting numbers of cells attached to each worm (n=6 per group, 3 replicate wells). Culture supernatants were collected for cytokine quantification by cytokine bead array, inflammation panel (Thermoscientific).

Statistical Analysis

Values are reported as means ± standard error of the mean (SEM). Multiple experiments were performed and combined for final data analysis, and data were analyzed by the unpaired t-test for 2-group comparison or one-way ANOVA for multiple groups comparison followed by post-Tukey or Dunnett's multiple comparison test where appropriate using Graphpad Prism 9 (Graphpad Software, La Jolla, CA). For data collected over several time points, two-way ANOVA with post-Tukey or Sidak's multiple comparison test was performed. Comparisons with P values less than 0.05 were considered statistically significant.

Supplementary Material

Refer to Web version on PubMed Central for supplementary material.

Acknowledgments

These studies were supported by the National Institutes of Health/NIAID (R01AI153195 to MGN; R01AI091759 to MGN and MB). The authors would like to thank David D. Lo for provision of the PGRPredCx3CR1GFP transgenic mice; Spencer H. Wang, Jessica C. Jang, and Hashini M. Batugedara for assistance with experiments; Holly Eckelhoefer and John Weger of the UC Riverside Genomics core (Riverside, CA) for assistance with cell sorting and RNA sequencing.

References

[1]. Hotez PJ, Brindley PJ, Bethony JM, King CH, Pearce EJ, Jacobson J, J Clin Invest 2008, 118, 1311. [PubMed: 18382743]

[2]. De Clercq D, Sacko M, Behnke J, Gilbert F, Dorny P, Vercruysse J, Am J Trop Med Hyg 1997, 57, 25; [PubMed: 9242313] Reynoldson JA, Behnke JM, Pallant LJ, Macnish MG, Gilbert F, Giles S, Spargo RJ, Thompson RC, Acta Trop 1997, 68, 301. [PubMed: 9492915]

[3]. Jia TW, Melville S, Utzinger J, King CH, Zhou XN, PLoS Negl Trop Dis 2012, 6, e1621; [PubMed: 22590656] Speich B, Moser W, Ali SM, Ame SM, Albonico M, Hattendorf J, Keiser J, Parasit Vectors 2016, 9, 123. [PubMed: 26935065]

[4]. Gause WC, Wynn TA, Allen JE, Nat Rev Immunol 2013, 13, 607. [PubMed: 23827958]

[5]. Weatherhead JE, Gazzinelli-Guimaraes P, Knight JM, Fujiwara R, Hotez PJ, Bottazzi ME, Corry DB, Front Immunol 2020, 11, 594520. [PubMed: 33193446]

[6]. Marsland BJ, Kurrer M, Reissmann R, Harris NL, Kopf M, Eur J Immunol 2008, 38, 479. [PubMed: 18203142]

[7]. Chen F, Wu W, Millman A, Craft JF, Chen E, Patel N, Boucher JL, Urban JF, Kim CC, Gause WC, Nat Immunol 2014, 15, 938. [PubMed: 25173346]

[8]. Bouchery T, Moyat M, Sotillo J, Silverstein S, Volpe B, Coakley G, Tsourouktsoglou TD, Becker L, Shah K, Kulagin M, Guiet R, Camberis M, Schmidt A, Seitz A, Giacomin P, Le Gros G, Papayannopoulos V, Loukas A, Harris NL, Cell Host Microbe 2020, 27, 277. [PubMed: 32053791]

[9]. Knott ML, Matthaei KI, Giacomin PR, Wang H, Foster PS, Dent LA, Int J Parasitol 2007, 37, 1367; [PubMed: 17555758] Voehringer D, Reese TA, Huang X, Shinkai K, Locksley RM, J Exp Med 2006, 203, 1435; [PubMed: 16702603] Giacomin PR, Gordon DL, Botto M, Daha MR, Sanderson SD, Taylor SM, Dent LA, Mol Immunol 2008, 45, 446. [PubMed: 17675237]

[10]. de Marcken M, Dhaliwal K, Danielsen AC, Gautron AS, Dominguez-Villar M, Sci Signal 2019, 12;Serbina NV, Jia T, Hohl TM, Pamer EG, Annu Rev Immunol 2008, 26, 421; [PubMed: 18303997] Hohl TM, Rivera A, Lipuma L, Gallegos A, Shi C, Mack M, Pamer EG, Cell Host Microbe 2009, 6, 470. [PubMed: 19917501]

[11]. Manta C, Heupel E, Radulovic K, Rossini V, Garbi N, Riedel CU, Niess JH, Mucosal Immunol 2013, 6, 177; [PubMed: 22854708] Choi JY, Kim JH, Hossain FMA, Uyangaa E, Park SO, Kim B, Kim K, Eo SK, Front Immunol 2019, 10, 1467. [PubMed: 31316515]

[12]. Freria CM, Hall JC, Wei P, Guan Z, McTigue DM, Popovich PG, J Neurosci 2017, 37, 3568; [PubMed: 28264978] Faustino J, Chip S, Derugin N, Jullienne A, Hamer M, Haddad E, Butovsky O, Obenaus A, Vexler ZS, J Cereb Blood Flow Metab 2019, 39, 1919. [PubMed: 30628839]

[13]. Ran L, Yu Q, Zhang S, Xiong F, Cheng J, Yang P, Xu JF, Nie H, Zhong Q, Yang X, Yang F, Gong Q, Kuczma M, Kraj P, Gu W, Ren BX, Wang CY, Dis Model Mech 2015, 8, 691. [PubMed: 26035381]

[14]. Cho JH, Fraser IP, Fukase K, Kusumoto S, Fujimoto Y, Stahl GL, Ezekowitz RA, Blood 2005, 106, 2551. [PubMed: 15956276]

[15]. Jung S, Aliberti J, Graemmel P, Sunshine MJ, Kreutzberg GW, Sher A, Littman DR, Mol Cell Biol 2000, 20, 4106. [PubMed: 10805752]

[16]. Wang J, Gusti V, Saraswati A, Lo DD, J Immunol 2011, 187, 5277. [PubMed: 21984701]

[17]. Camberis M, Le Gros G, Urban J, Curr Protoc Immunol 2003, Chapter 19, Unit 19.12.

[18]. Stein M, Keshav S, Harris N, Gordon S, J Exp Med 1992, 176, 287. [PubMed: 1613462]

[19]. Hussell T, Bell TJ, Nat Rev Immunol 2014, 14, 81; [PubMed: 24445666] Aegerter H, Kulikauskaite J, Crotta S, Patel H, Kelly G, Hessel EM, Mack M, Beinke S, Wack A, Nat Immunol 2020, 21, 145. [PubMed: 31932810]

[20]. Batugedara HM, Li J, Chen G, Lu D, Patel JJ, Jang JC, Radecki KC, Burr AC, Lo DD, Dillman AR, Nair MG, J Leukoc Biol 2018.

[21]. Iyer AK, Liu J, Gallo RM, Kaplan MH, Brutkiewicz RR, Immunology 2015, 146, 444; [PubMed: 26260288] Marti F, Post NH, Chan E, King PD, J Exp Med 2001, 193, 1425; [PubMed: 11413197] Sagebiel AF, Steinert F, Lunemann S, Körner C, Schreurs RRCE, Altfeld M, Perez D, Reinshagen K, Bunders MJ, Nat Commun 2019, 10, 975. [PubMed: 30816112]

[22]. Rogers ML, Bailey S, Matusica D, Nicholson I, Muyderman H, Pagadala PC, Neet KE, Zola H, Macardle P, Rush RA, J Neuroimmunol 2010, 226, 93; [PubMed: 20547427] Salehi AH, Xanthoudakis S, Barker PA, J Biol Chem 2002, 277, 48043. [PubMed: 12376548]

[23]. Zhan Y, Brown C, Maynard E, Anshelevich A, Ni W, Ho IC, Oettgen P, J Clin Invest 2005, 115, 2508; [PubMed: 16138193] Stamatovic SM, Keep RF, Mostarica-Stojkovic M, Andjelkovic AV, J Immunol 2006, 177, 2651. [PubMed: 16888027]

[24]. Frishberg A, Brodt A, Steuerman Y, Gat-Viks I, Bioinformatics 2016, 32, 3842. [PubMed: 27531105]

[25]. Yang R, Wang M, Zhang G, Li Y, Wang L, Cui H, Cell Death Dis 2021, 12, 433. [PubMed: 33931589]

[26]. Coletta S, Salvi V, Della Bella C, Bertocco A, Lonardi S, Trevellin E, Fassan M, D'Elios MM, Vermi W, Vettor R, Cagnin S, Sozzani S, Codolo G, de Bernard M, Sci Rep 2020, 10, 16501. [PubMed: 33020563]

[27]. Bernstein KE, Khan Z, Giani JF, Cao DY, Bernstein EA, Shen XZ, Nat Rev Nephrol 2018, 14, 325. [PubMed: 29578208]

[28]. Kang D, Liu G, Lundström A, Gelius E, Steiner H, Proc Natl Acad Sci U S A 1998, 95, 10078. [PubMed: 9707603]

[29]. Tydell CC, Yount N, Tran D, Yuan J, Selsted ME, J Biol Chem 2002, 277, 19658. [PubMed: 11880375]

[30]. Imai T, Hieshima K, Haskell C, Baba M, Nagira M, Nishimura M, Kakizaki M, Takagi S, Nomiyama H, Schall TJ, Yoshie O, Cell 1997, 91, 521; [PubMed: 9390561] Charo IF, Myers SJ, Herman A, Franci C, Connolly AJ, Coughlin SR, Proc Natl Acad Sci U S A 1994, 91, 2752. [PubMed: 8146186]

[31]. Lee J, Boyce S, Powers J, Baer C, Sassetti CM, Behar SM, PLoS Pathog 2020, 16, e1008621; [PubMed: 32544188] Shin KS, Jeon I, Kim BS, Kim IK, Park YJ, Koh CH, Song B, Lee JM, Lim J, Bae EA, Seo H, Ban YH, Ha SJ, Kang CY, Front Immunol 2019, 10, 1887. [PubMed: 31474983]

[32]. Bonduelle O, Duffy D, Verrier B, Combadière C, Combadière B, J Immunol 2012, 188, 952. [PubMed: 22219332]

[33]. Lin KL, Suzuki Y, Nakano H, Ramsburg E, Gunn MD, J Immunol 2008, 180, 2562. [PubMed: 18250467]

[34]. Geissmann F, Jung S, Littman DR, Immunity 2003, 19, 71. [PubMed: 12871640]

[35]. Shi C, Pamer EG, Nat Rev Immunol 2011, 11, 762; [PubMed: 21984070] Francis M, Groves AM, Sun R, Cervelli JA, Choi H, Laskin JD, Laskin DL, Toxicol Sci 2017, 155, 474. [PubMed: 27837169]

[36]. Amsellem V, Abid S, Poupel L, Parpaleix A, Rodero M, Gary-Bobo G, Latiri M, Dubois-Rande JL, Lipskaia L, Combadiere C, Adnot S, Am J Respir Cell Mol Biol 2017, 56, 597. [PubMed: 28125278]

[37]. Leonardi I, Li X, Semon A, Li D, Doron I, Putzel G, Bar A, Prieto D, Rescigno M, McGovern DPB, Pla J, Iliev ID, Science 2018, 359, 232. [PubMed: 29326275]

[38]. Ishida Y, Kimura A, Nosaka M, Kuninaka Y, Hemmi H, Sasaki I, Kaisho T, Mukaida N, Kondo T, Sci Rep 2017, 7, 16833. [PubMed: 29203799]

[39]. Beresford PJ, Zhang D, Oh DY, Fan Z, Greer EL, Russo ML, Jaju M, Lieberman J, J Biol Chem 2001, 276, 43285; [PubMed: 11555662] Fan Z, Beresford PJ, Oh DY, Zhang D, Lieberman J, Cell 2003, 112, 659; [PubMed: 12628186] Fan Z, Beresford PJ, Zhang D, Xu Z, Novina

CD, Yoshida A, Pommier Y, Lieberman J, Nat Immunol 2003, 4, 145; [PubMed: 12524539] Martinvalet D, Zhu P, Lieberman J, Immunity 2005, 22, 355; [PubMed: 15780992] Zhang D, Pasternack MS, Beresford PJ, Wagner L, Greenberg AH, Lieberman J, J Biol Chem 2001, 276, 3683. [PubMed: 11060286]

[40]. Elavazhagan S, Fatehchand K, Santhanam V, Fang H, Ren L, Gautam S, Reader B, Mo X, Cheney C, Briercheck E, Vasilakos JP, Dietsch GN, Hershberg RM, Caligiuri M, Byrd JC, Butchar JP, Tridandapani S, J Immunol 2015, 194, 2786. [PubMed: 25667415]

[41]. Zhang M, Park SM, Wang Y, Shah R, Liu N, Murmann AE, Wang CR, Peter ME, Ashton-Rickardt PG, Immunity 2006, 24, 451. [PubMed: 16618603]

[42]. Fujiwara A, Kawai Y, Sekikawa S, Horii T, Yamada M, Mitsufuji S, Arizono N, J Parasitol 2004, 90, 1019. [PubMed: 15562601]

[43]. Hartmann W, Marsland BJ, Otto B, Urny J, Fleischer B, Korten S, J Immunol 2011, 186, 2472. [PubMed: 21248253]

[44]. Langmead B, Salzberg SL, Nat Methods 2012, 9, 357; [PubMed: 22388286] Kim D, Pertea G, Trapnell C, Pimentel H, Kelley R, Salzberg SL, Genome Biol 2013, 14, R36. [PubMed: 23618408]

[45]. Lawrence M, Huber W, Pagès H, Aboyoun P, Carlson M, Gentleman R, Morgan MT, Carey VJ, PLoS Comput Biol 2013, 9, e1003118. [PubMed: 23950696]

[46]. Robinson MD, McCarthy DJ, Smyth GK, Bioinformatics 2010, 26, 139. [PubMed: 19910308]

[47]. Mortazavi A, Williams BA, McCue K, Schaeffer L, Wold B, Nat Methods 2008, 5, 621. [PubMed: 18516045]

[48]. Huang d. W., Sherman BT, Lempicki RA, Nucleic Acids Res 2009, 37, 1. [PubMed: 19033363]

[49]. Esser-von Bieren J, Mosconi I, Guiet R, Piersgilli A, Volpe B, Chen F, Gause WC, Seitz A, Verbeek JS, Harris NL, PLoS Pathog 2013, 9, e1003771. [PubMed: 24244174]

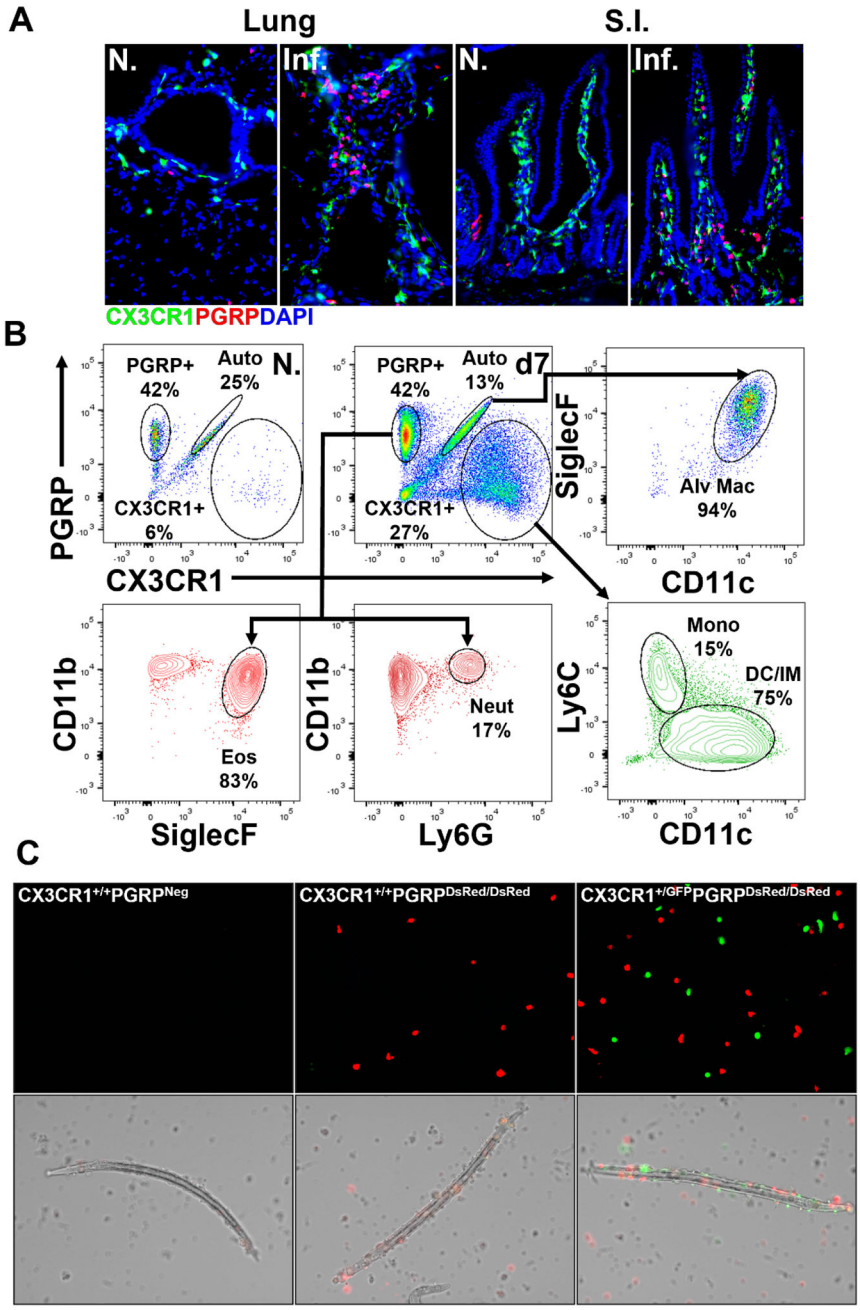

Figure 1. ***Nippostrongylus*** **infection induces lung infiltration of CX3CR1^{+} myeloid cells and PGRP^{+} eosinophils.**

CX3CR1$^{+/GFP}$/PGRP^{dsRED} transgenic mice were infected with 500 L3 Nb, followed by analysis of lung and blood at day 7 post-infection. **(A)** CX3CR1-GFP and PGRP-DsRed signal in frozen lung and small intestine (S.I.) sections. **(B)** Temporal changes in CX3CR1 and PGRP cell populations were assessed by flow cytometry. **(C)** Lung cells were isolated from CX3CR1$^{+/+}$PGRP^{Neg}, CX3CR1$^{+/+}$PGRP^{DsRed}, and CX3CR1$^{+/GFP}$PGRP^{DsRed} mice at 7 days post-infection, and co-cultured with *Nb* L3 larvae. Data are representative of 2 experiments in (A and B) and of 1 experiment in (C).

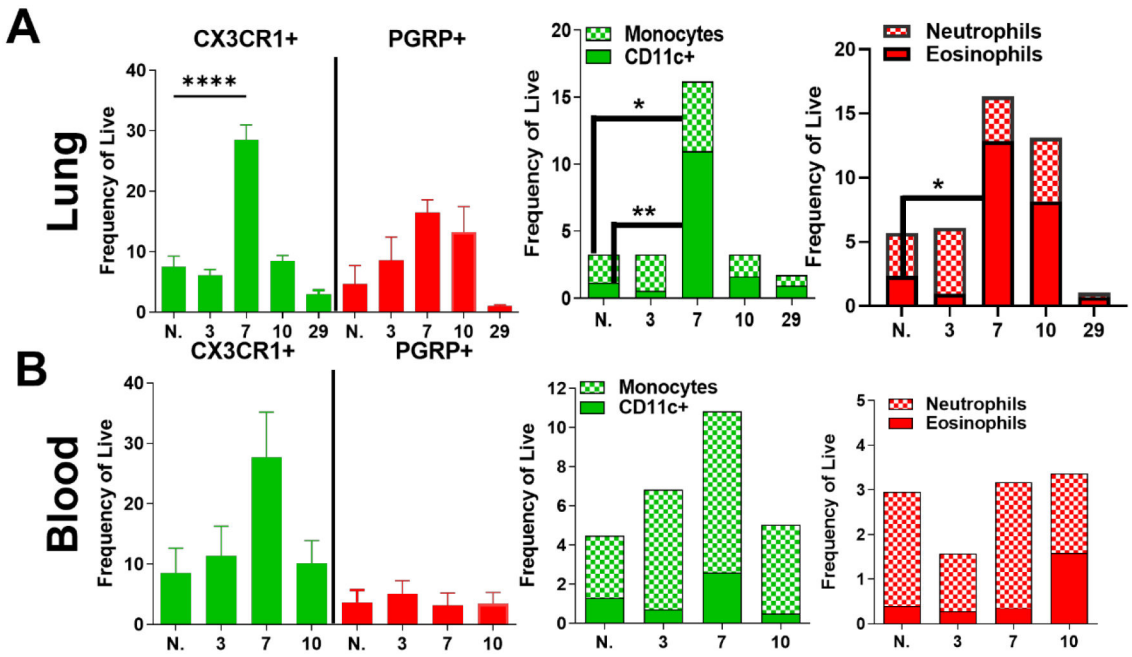

Fig 2. The recruitment of CX3CR1+ monocytes and CD11c+ cells peaked at day 7 post-infection.

$CX3CR1^{+/GFP}/PGRP^{DsRed}$ transgenic mice were infected with 500 Nb L3, followed by analysis of lung and blood at various time points post-infection. **(A-B)** CX3CR1 and PGRP populations and subpopulations were quantified in (A) the lung and (B) blood. Values represent means ± SEM (n = 3–6 animals per time point), and data are representative of 2 experiments. One-way ANOVA with Dunnett's multiple comparison test and two-way ANOVA with post-Tukey multiple comparison test were performed, and P values less than 0.05 were considered statistically significant. (*, P≤0.05; **, P≤0.01; ***, P≤0.001; ****, P≤0.0001)

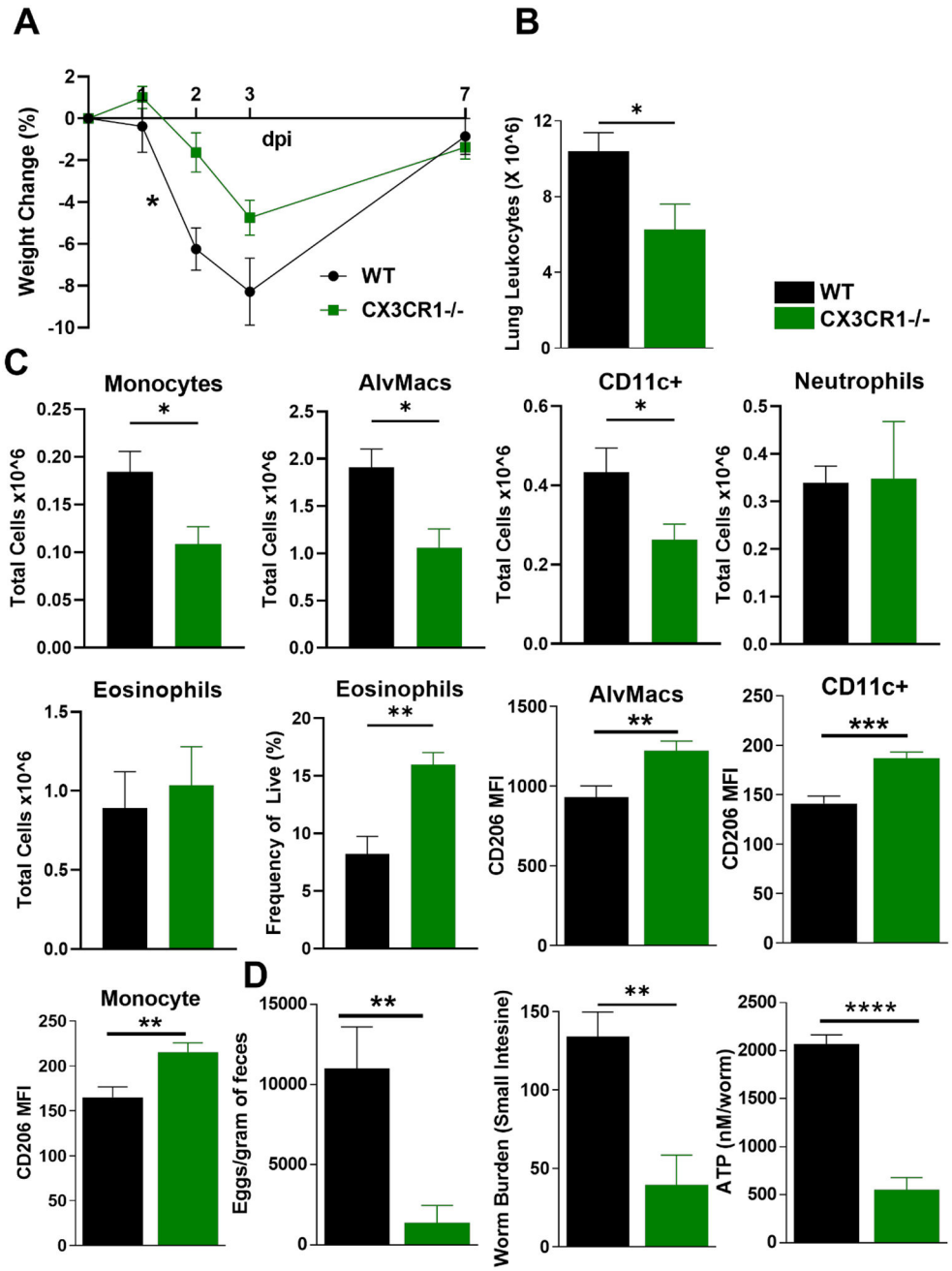

Figure 3. CX3CR1 deficiency reduces Nippostrongylus parasite burden and decreases infection-induced weight loss and lung leukocyte infiltration.

CX3CR1 wild-type (WT) or CX3CR1$^{GFP/GFP}$ (−/−) mice were infected subcutaneously with 500 *Nippostrongylus* L3. **(A)** Infection-induced weight loss compared to pre-infection weight was calculated at multiple time points. **(B)** Total lung leukocytes were enumerated. **(C)** Myeloid and granulocyte subsets were determined and CD206 median fluorescence intensity (MFI) in alveolar macrophages, monocytes and CD11c^{+} lung cells were evaluated by flow cytometry. **(D)** Parasite burden was evaluated at day 7 post-infection by fecal egg count, intestinal worm count and measurement of worm viability by ATP quantification of

adult worms dissected from the small intestine. Values represent means ± SEM (n = 6–7 per group), and data is representative of 3 experiments. Two-way ANOVA with post-Sidak multiple comparison test and the unpaired t-test were performed, and P values less than 0.05 were considered statistically significant. (*, P≤0.05; **, P≤0.01; ***, P≤0.001; ****, P≤0.0001)

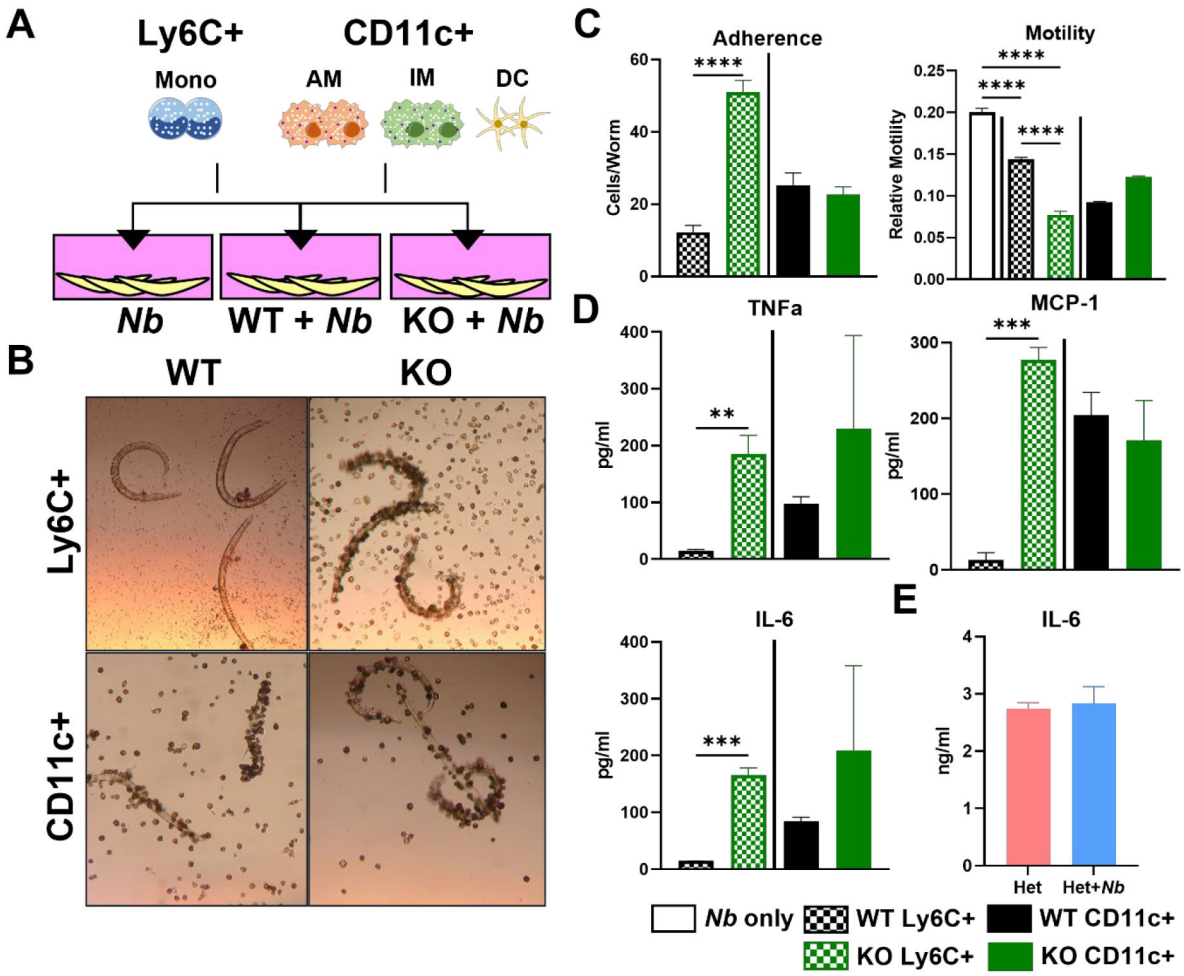

Figure 4. CX3CR1-deficient Ly6c+ monocytes secrete more proinflammatory cytokines and actively bind *Nippostrongylus* L3 parasites.

(A) Schematic representation of magnetic assisted cell sorting (MACs) of cells from CX3CR1 wild-type (WT) and CX3CR1$^{GFP/GFP}$ (KO) *Nippostrongylus*-infected lungs, and co-culture with L3 *Nippostrongylus* parasites. **(B)** Representative micrographs of Ly6c+ and CD11c+ cells from WT or KO mice adhered to L3 Nb. **(C)** Cellular adherence and relative *Nippostrongylus* motility were assessed at day 3 co-culture. **(D)** Cytokines and chemokines in WT and KO cell co-culture medium were measured. **(E)** IL-6 secretion by lung cells isolated from *Nippostrongylus*-infected CX3CR1$^{+/GFP}$PGRP^{DsRed} (Het) mice cultured with or without *Nippostrongylus* larvae. Values represent means ± SEM (n = 5 animals, n = 3–4 for cell culture replicates) and are representative of 3 experiments in (C and D) and 1 experiment in (E). The unpaired t-test was performed, and P values less than 0.05 were considered statistically significant. (*, P≤0.05; **, P≤0.01; ***, P≤0.001; ****, P≤0.0001)

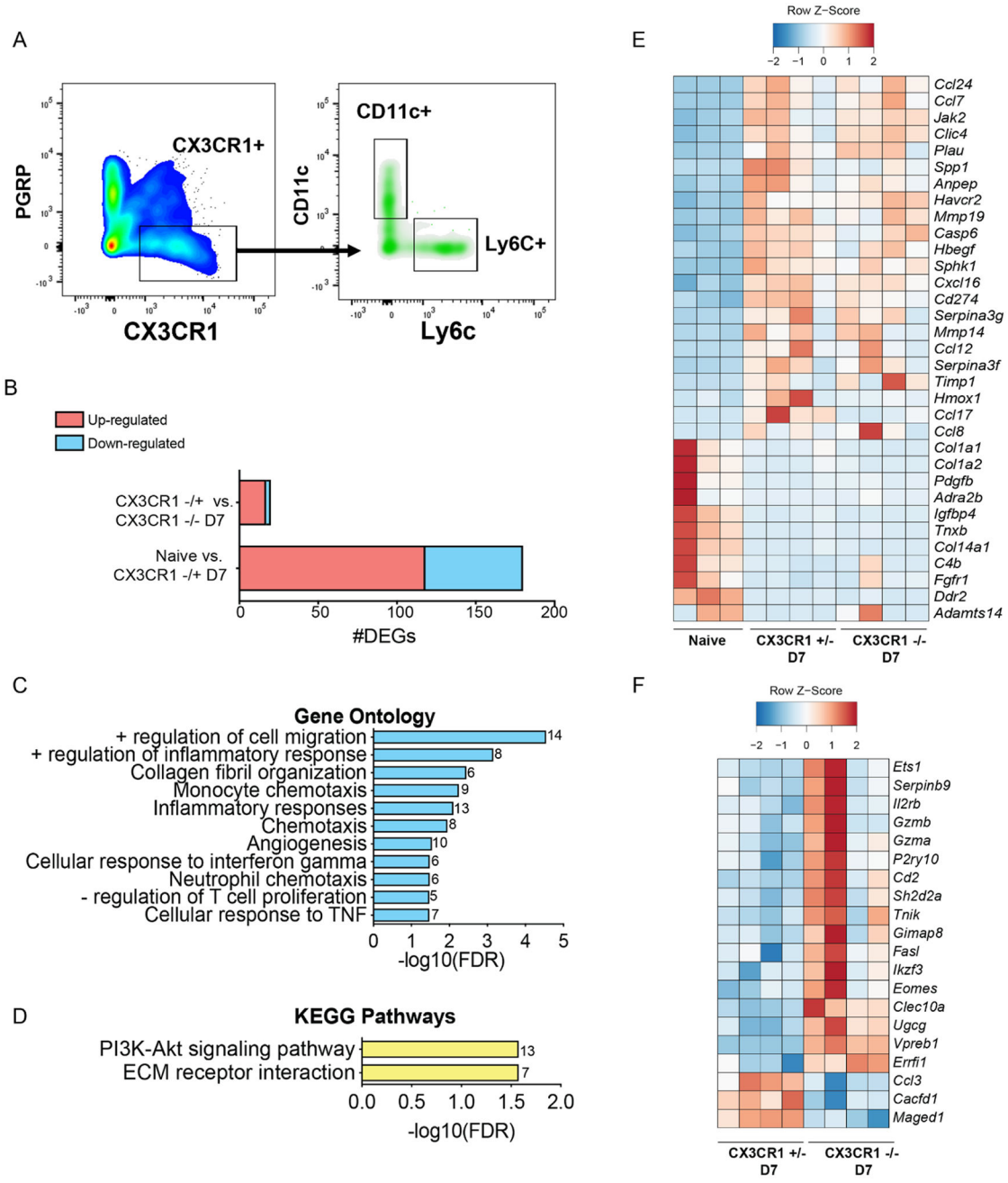

Figure 5. RNA-sequencing analysis of lung Ly6C+ monocytes sorted from naive and infected CX3CR1$^{+/GFP}$ (Het) and Cx3CR1$^{GFP/GFP}$ (KO) mice.

CX3CR1$^{+/GFP}$PGRP^{DsRed} (Het) were injected with PBS control (naive) or infected with *Nippostrongylus* for 7 days, and compared to day 7-infected Cx3CR1$^{GFP/GFP}$ PGRP^{DsRed} (KO) mice. **(A)** Ly6c+ and CD11c+ cells within the live, single cell-gated CX3CR1 GFP+ cell populations were recovered via flow cytometry-assisted cell sorting from lung leukocytes of naïve CX3CR1$^{+/GFP}$ or infected CX3CR1$^{+/GFP}$ and CX3CR1$^{GFP/GFP}$ mice. **(B)** Bar graph summarizing transcriptional changes in monocytes - naïve CX3CR1$^{+/GFP}$ vs. infected CX3CR1$^{+/GFP}$ and infected CX3CR1$^{+/GFP}$ vs. CX3CR1$^{GFP/GFP}$ mice. X axis represents number of significantly different genes (log2 FC ≥ 1 and FDR ≤ 5%)

up-regulated (red) or down-regulated (blue) under each comparison **(C-D)** Bar graphs representing functional enrichment – **(C)** Gene Ontologies (GO) and **(D)** KEGG pathways of differentially expressed genes within the naïve CX3CR1$^{+/GFP}$ group. Ontologies were predicted using DAVID (FDR ≤ 5%). Number of genes mapping to each term is annotated. **(E)** Clustered heatmap of DEGs discovered in naïve vs. infected CX3CR1$^{+/GFP}$ mapping to GO terms “inflammatory response”, “regulation of cell migration”, and “collagen fibril organization”. **(F)** Clustered heatmap of DEGs discovered when comparing CX3CR1$^{GFP/GFP}$ to CX3CR1$^{+/GFP}$ Ly6c+ (F). n = 3–4 per group from one experiment.